

# Sharp Tactile Sensation using Superposition of Vibrotactile Stimuli in Different Phases

Tatsuma Sakurai, Hiroyuki Shinoda, Masashi Konyo

The University of Tokyo, The University of Tokyo, Tohoku University

## ABSTRACT

The overlapping of vibrations that are in different phases and in close proximity to each other produces a tactile image that is more localized than one produced by pin vibrators. The mechanism behind the former is still unclear; it may be attributed to the fact that the resultant vibration is highly localized and of a high frequency, making the tactile sensations more perceptible by the human hand. In this study, a finite element (FE) model of a human finger is analyzed to investigate the reason for the difference in the sizes of tactile images produced under different mechanical conditions. In the dynamic analysis, we observed the spatial distribution of the strain energy density (SED) in the model and estimated the perceptual area of the mechanical stimuli. To determine the perceptual area, the threshold SED for perceiving the vibratory stimuli was determined by analyzing the FE finger model on a flat vibratory surface. In the deformation analysis results, we observed that the spatial distribution of SED was more localized by the overlapped vibrations than in a pin vibrator. Moreover, spectral analysis revealed that a higher-frequency vibration was generated locally between the two vibrations. A psychophysical experiment was conducted to determine the effect of the high frequency component on detection thresholds.

**KEYWORDS:** haptics, vibrotactile stimulation.

**INDEX TERMS:** H.5.2 [Information Interfaces and Presentation]: User Interfaces—Haptic I/O, H.1.2 [Models and principles]: User/Machine Systems—Human factors

## 1 INTRODUCTION

Surface shape production techniques that utilize haptic feedback have been in great demand owing to the proliferation of touch panels and other touch-controlled electronic devices. Haptic perception of surface shapes provides important cues for detecting edges, lines, and other geometric information such as a letter or symbol. Moreover, it facilitates intuitive handling in virtual interactions.

Since humans are highly sensitive to vibrations, haptic perception is generally exploited by supplying vibratory stimuli to the skin. This method is known as vibrotactile stimulation and the stimuli are generated by vibrators or electrodes.

Haptic displays are generally equipped with a large array of vibrators, which vibrate independently and combine all the many dot-shaped sensations that they individually generate into a single tactile shape. To transmit more tactile information, higher spatial resolution stimuli are used. Recently, many haptic displays have been developed for the transmission of high-spatial-resolution tactile information. For example, the optical-to-tactile converter

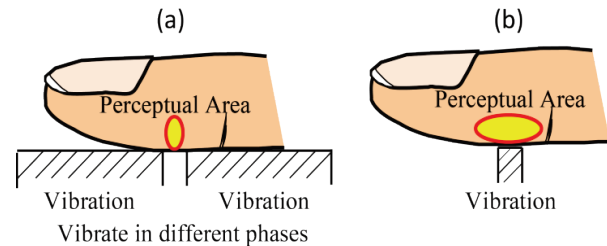


Figure 1. (a). Vibration overlap method. Two surfaces of square vibrators in close proximity are vibrating in different phases with detection threshold level amplitudes and human perceive sharp tactile sensation between above the gap of them.

(b). Pin vibrator. We define Pin as thin pole with a diameter of 0.5mm in this thesis. Tactile image becomes wide spread and the tactile image gets blurry.

(Optacon) is a Braille display that produces tactile images by combining several dot patterns [1], with each vibrotactile dot sensation produced by pin-shaped vibrators. Not only Braille dots but also surface shapes can be produced from the information obtained by the image sensor. Summers et al. developed a tactile array display comprising 100 contactors in a  $1 \times 1$  cm matrix [2]. Paul et al. developed a 49-point  $1.8 \times 1.8$  cm electrotactile display for use with the fingertip (electrotactile displays produce electrical stimulations) produced by means of a matrix of electrodes that apply small and controlled electric currents to a touch-sensitive area such as the skin or tongue [3]. Kyung et al. developed a high-performance  $6 \times 5$  tactile display actuated by piezoelectric bimorphs [4]. Furthermore, Yang et al. developed a miniature pin-array tactile module that utilizes elastic and electromagnetic forces. The module had nine 0.5-mm-diameter contactors spaced at 3.0 mm. Stress2 is another haptic display that uses lateral vibrations of a piezoelectric vibrator to generate dot-shaped tactile information [5], while VITAL is an  $8 \times 8$  matrix (2 mm spacing) vibrotactile display [6] and  $3 \times 3$  matrix tactile display developed by Yang [7].

Most of these haptic displays were equipped with pin vibrators arranged in an array approximately at intervals of two-point discrimination (2 mm) or higher densities. However, pin-array devices have limited spatial resolutions. Irrespective of the partiality of the vibrotactile stimulus, the radial skin deformation caused by a single pin vibrator activates a wider area of mechanoreceptors, leading to the production of tactile images that are blurrier and with wider spreads. With such blurry images, it is difficult to obtain high-resolution tactile information. Thus, to achieve higher spatial resolutions, it is essential to trigger the mechanoreceptors as localized as possible.

Instead of pin vibrators, we propose the use of an array of square shape vibrators, which are vibrated in different phases and very small amplitudes. We call this as the vibration overlap method [8][9]. Fig. 1(a) is a schematic of the vibration overlap method. Through the use of square shape vibrators and small amplitudes vibratory stimuli, skin deformation can be suppressed and sharp and clear tactile sensations can be perceived in the gaps

Tatsuma Sakurai and Hiroyuki Shinoda: Graduate School of Information Sciences and Technology, The University of Tokyo, 7-3-1 Hongo, Bunkyo-ku, Tokyo, Japan  
Masashi Konyo: Graduate School of Information Sciences, Tohoku University, 6-6-01 Aramaki Aza Aoba, Aoba-ku, Sendai, Japan

IEEE World Haptics Conference 2013  
14-18 April, Daejeon, Korea  
978-1-4799-0088-6/13/\$31.00 ©2013 IEEE

between the vibrators rather than on the square vibrators. To achieve high resolution gap, the square elements must be made small and those elements vibrating in the same phase can be count as the large area square elements.

As implied earlier, the detection threshold of a vibratory stimulus is significantly lower than that of a simple vibratory surface (Fig. 1(b)) correlated to the phase deviation of two vibrations and spatial distribution of those vibratory stimuli [9]. As shown in Fig. 1(a), we have found that the tactile image width (horizontal perceptual area in brain) produced by the vibration overlap method is smaller than those of pin vibrators. In concrete, a 0.5-mm-diameter pin vibrator with the amplitude of the detection threshold produces a 2.34-mm tactile image width. In contrast, the vibration overlap method with a gap of 0.5 mm produces a 0.64-mm tactile image width. The increase of amplitude also changes the width and the main effects are enhancing the sensational intensity and the tactile image width tendencies among the methods do not change. Previous pin-array tactile display can also generate vibrations in different phases; however they did not focus on the mechanical structure and stimuli conditions of vibration overlap method in the following two aspects.

**Mechanical structure:** The gap distance between vibrators must be in close proximity for a sharp tactile sensation (smaller the sharper), since the tactile sensation generates above the gap not above the vibrator itself in vibration overlap method. Though the previous pin-array vibrators are high dense, they are thin poles and sparse in areas.

**Vibratory stimuli:** The phases of vibrations must be carefully selected and the vibratory amplitude must be small under detection threshold level for the sharp sensation that generates at the gap of vibrators rather than on the vibrator itself. Vibrotactile stimuli in the previous works are large enough to be perceived.

By focusing on the several points described above, array-vibrator haptic displays can produce shaper, high intensity tactile sensations. The sharp tactile sensation generated by the vibration overlap method is useful for high-resolution, high-density tactile display. However, the mechanism by which the sharp tactile images of the vibration overlap method are produced remains unclear in the past works. The objective of our study is to determine the reason why tactile image widths differ for different boundary conditions. In particular, we investigate the mechanisms of perceptual area spreading of pin vibrators and the vibration overlap method.

When investigating the mechanisms of tactile images, we focus on the spatial deformation of the skin and the spatial distribution of deformation frequencies by vibratory stimuli. We conduct several deformation analyses of a finite element (FE) finger model and observe the spatial deformation around the pin and in the gap between two vibratory surfaces. Since the human sensitivity to vibratory stimuli differs in correspondence to the frequency, the spatial distribution of frequencies is also a key parameter for the perceptual area. If a higher-frequency vibration is aroused in a localized area, a human would be sensitive to that area. We conduct spectral analyses to investigate the frequencies that are dominant in a spatial area. We compare the spatial deformation of vibratory stimuli and spatial distributions of frequencies between a pin vibrator and the vibration overlap method. We estimate the actual perceptual area by determining several threshold deformations for vibratory stimuli at several frequencies (humans can perceive vibration beyond the threshold deformation) and compare those thresholds to deformation analysis results. Lastly, we conduct a psychophysical test to investigate the effects of the spatial distribution of frequencies on

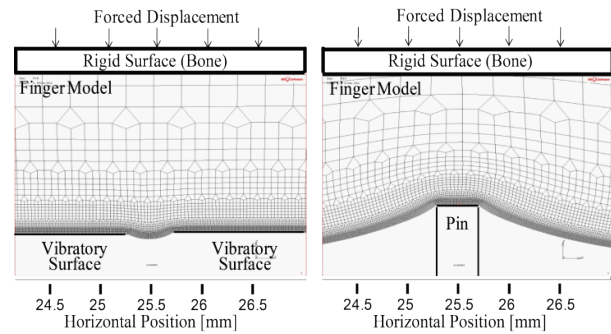


Figure 2. Finger model and other mechanical conditions. (a) Left: Vibration overlap method (0.5 mm gap). (b) Right: Pin-shaped vibrator (0.5 mm diameter).

Table 1. Mechanical parameters of finger model [11]

Depth from Surface [mm]	Young's Modulus [MPa]	Poisson's Ratio	Density [kg/mm <sup>3</sup> ]
0.0-0.05	0.680	0.48	1.1e-6
0.05-0.3	0.136	0.48	1.1e-6
0.3-0.6	0.085	0.48	1.1e-6
0.6-8.0	0.034	0.48	9.6e-7

Table 2. Conditions of the analyses

	Condition 1	Condition 2	Condition 3
Model	<b>Vibration Overlap</b>	<b>Pin Vibrator</b>	<b>Vibration Overlap</b>
Vibration Equations	eq. (1) + eq. (2)	eq. (1)	eq. (1) + eq. (2)
Frequency	30 Hz	60 Hz	30 Hz
Amplitude	10 um (same as Pin Vibrator)	10 um (detection threshold level)	5 um (detection threshold level)

detection thresholds.

## 2 PERFORMANCE OF VIBRATION OVERLAP METHOD

When the vibrators are in close proximity and vibrating in opposite phases, the boundary condition of those vibrators and skin changes by time, and the frequency of the resultant vibration is doubled partially in the gap between two surfaces and the minimum detection threshold is one-sixth that of simply touching a vibratory surface.

In previous study, it is indicated that vibrations overlap of 30 Hz vibratory stimuli in opposite phases provides same tactile sensation as 60 Hz (doubled frequency) stimuli by flat surface vibrator [8]. And it is also indicated that the detection thresholds behavior toward the gap distance parameter cannot be explained only by the linear frequency component of the stimuli but by the doubled frequency component generated between the vibrations. We have obtained these facts that the existences of doubled frequency component in the vibration overlap method affects to our tactile perception for vibratory stimuli. However, the doubled frequency component effects on perceptual area have not been discussed in our previous study. Therefore in this study, we focused on the performance of doubled frequency components in order to investigate the mechanism for different tactile images in addition to observe the skin deformation.

## 3 INVESTIGATION ON THE SPATIAL DISTRIBUTION OF STRAIN ENERGY DENSITY INSIDE FINGER MODEL

Tactile sensations differ according to the boundary conditions of the mechanical contacts between the skin and the vibrators. In this

section, we discuss the deformation analysis that we conducted on a finger model to observe the spatial distribution of the strain energy density (SED).

Stress and strain energies are positively correlated and previous studies have also indicated a correlation between the SED and vibrotactile sensation. For example, Srinivasan analyzed the human perception mechanism of a cylindrical model indented with rectangular gratings. In our study, the maximum compressive strain and SED at typical receptor locations emerged as two strain measures that were directly related to the electrophysiologically recorded response rate of slowly adapting type 1 (SA I) mechanoreceptors [10]. Srinivasan concluded that SED was a better candidate for the relevant stimulus of SA I receptors since, it is a scalar that is invariant with respect to the orientation of the receptor and is a direct measure of the distortion of the receptor caused by the loads imposed on the skin. In addition, Maeno et al. constructed an FE model of the human finger by measuring its geometry and the material properties of its tissue [11]. They concluded that there was a linear relationship between the SED of the tactile receptors and the firing frequency of the nerve impulse. Makino also investigated the spatial distribution of the SED inside an FE model of a finger [12]. They suggested that similar SED distributions inside the finger produced the same tactile sensation. In their study, a static suction sensation generated by a small cylindrical hole produced the same sensation as done by the pressure applied by a pin of the same size as the suction hole.

Therefore, we used the SED of the finger to compare the perceptual area created by vibratory deformation under several conditions. By analyzing the spatial distribution of the SED and the spatial distribution of the frequencies of the SED, we investigated the effects of the mechanical structure and stimuli conditions on the tactile image width.

### 3.1 Model and Method

Fig. 2 shows the finger model simulated in our study. Since our focus was not on the absolute values of the SED but on the spatial distribution of the SED inside the finger model, the FE model developed in this study had a simple 2D rectangular shape. The largest mesh size was  $2.0 \text{ mm}^2$ , which was used around the top of the finger model. The smallest mesh size was  $10.0 \text{ mm}^2$  and appeared around the bottom of the model. The height of the model was 8.0 mm (the average distance from the surface of the human skin to the peripheral bone) and the width was 51.2 mm. These dimensions were large enough to eliminate the effects of the side boundaries. The first layer of the model (0.00–0.05 mm deep) represented the horny layer; the second layer (0.05–0.30 mm) represented the epidermis; the third layer (0.30–0.60 mm) represented the dermis; and the last layer (0.60–8.00 mm) represented the subcutis. Table 1 lists the parameters of the finger model; the Young's modulus, Poisson's ratio, and density of each layer were taken from Maeno's work [11]. In our study, we used vibratory stimuli of about 30–60 Hz, to which Meissner's disk is most sensitive. Since Meissner's disk exists in the boundary between the epidermis and the dermis, we observed the SED at a depth of 0.05 mm below the surface of the skin.

There were two rigid surfaces of 30mm each under the contacting finger model as shown in Fig. 2(a), both of which were vibratory surfaces with forced displacement. Both surfaces were in friction contact with the finger model and the former was able to peel off from the latter. The gap between the two surfaces was set to 0.5 mm, which was the same as in previous works that investigated the tactile image width. The pin vibrator, shown in Fig. 2(b), had rigid rectangular surfaces and the narrow side was set to 0.5 mm. There was also a rigid surface on the top of the model, glued to the finger by a zero fixed displacement and representing the rigid bone of the finger.

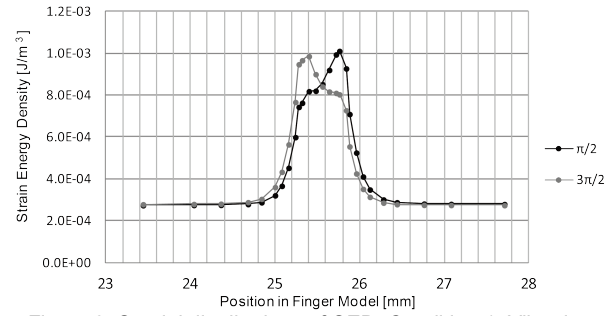


Figure 3. Spatial distributions of SED. Condition 1: Vibration overlap with  $10 \mu\text{m}$  amplitude.

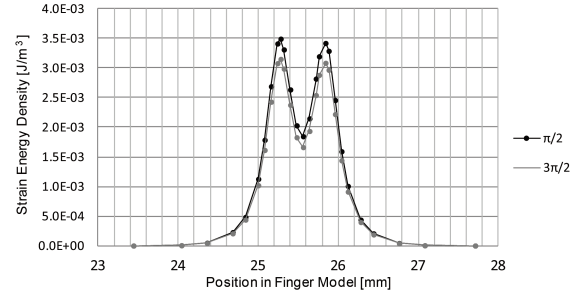


Figure 4. Spatial distributions of SED. Condition 2: Pin-type vibrator with  $10 \mu\text{m}$  amplitude.

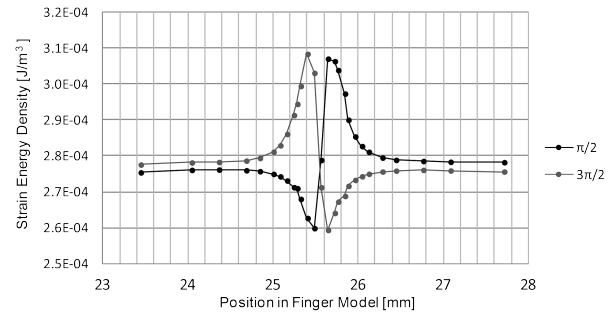


Figure 5. Spatial distributions of SED. Condition 3: Vibration overlap with  $5 \mu\text{m}$  amplitude.

In the dynamic analysis, the vibratory surfaces moved according to the following equations:

$$y(t) = A \sin(2\pi ft) \quad (1)$$

$$y(t) = A \sin(2\pi ft + \phi) \quad (2)$$

where  $y(t)$  is the deformation of the vibrators [ $\mu\text{m}$ ],  $A$  is the amplitude [ $\mu\text{m}$ ],  $f$  is the frequency [Hz], and  $\Phi$  is the phase deviation.

We used opposite phases for the vibration overlap, so  $\Phi = \pi$ . Table 2 shows the vibratory conditions used in this analysis. Condition 1 corresponds to the vibration overlap with the vibratory surfaces in opposite phase at 30 Hz. The amplitude was the same as that of the pin vibrator. Condition 2 corresponds to the pin vibrator with a frequency of 60 Hz. The amplitude was set to the detection threshold level of  $10 \mu\text{m}$ . Condition 3 also corresponds to the vibration overlap but with the amplitude set to the detection threshold level of  $5 \mu\text{m}$ . The analysis time was 0.5 s, with 10000 increments. The rigid bone moved down by 0.8 mm, which is equivalent to a 1 N pressure force. The rigid bone moved during the initial 0.1 s and the vibration started at 0.15 s. The analysis time was long enough for the stability of the dynamic analysis.

### 3.2 Result1: Spatial distributions of SED

Fig. 3, Fig. 4, and Fig. 5 show the spatial distributions of the SED at  $\pi/2$  and  $3\pi/2$ . Under condition 1, the SED peaked in both cases at the edge of the vibratory surfaces. Under condition 2, the SED peaked at the edge of the pin corner at  $\pi/2$ ; this was the highest absolute value of the SED and was due to the stress concentration at the edge. Compared SED peak to Condition 1, though amplitude is the same, the peak is three times larger. Although the absolute value of the SED under condition 3 was lower than that under condition 1, other spatial tendencies were almost the same in both cases.

### 3.3 Result2: Spatial distributions of SED amplitudes

According to the deformation analysis results, the absolute value of SED was highest under Condition 2. However, the important information is the amplitude of the change in SED (difference between the maximum and minimum) rather than the absolute value of SED, because the deformation is caused by the vibratory stimuli. Therefore, the SED amplitude was a better candidate for comparing the deformations caused by vibratory stimuli. Thus, we used the SED amplitude as an index to compare deformations.

We calculated the SED amplitude by subtracting the maximum SED from the minimum SED selected from the direction of the time axis at every horizontal sample point. The results are shown in Figs. 6(a), 7(a), and 8(a). Comparison of the curves of the SED amplitudes revealed that the pin condition had the widest base width, which means that the deformation of the vibratory stimuli spread. Under Condition 1, the SED amplitude spread was still smaller than that in Condition 2, which means that even the amplitude of the vibration was the same; the SED amplitude spatial distribution was localized significantly with the vibration overlap method. Under Condition 3, the SED amplitude is more localized than any other conditions.

### 3.4 Linear and Doubled Frequency Components

SED amplitude has no information for time component, so we also conducted the spectral analysis in order to investigate the frequency of deformation. We observed the frequency component of the change in SED at each sample point. We categorized the frequency component into two parts: frequencies around linear components (30–45 Hz) of the stimuli and those at doubled frequency (60–75 Hz).

Figs. 6(b), 7(b), and 8(b) show the spectral analysis results. Under Condition 1, in almost every position, the linear component was dominant. At the very center of the gap, the power spectral density (PSD) of the doubled frequency component was almost the same as that of the linear component. This was due to the vibration overlap of the two opposite-phased vibrations, and evidence for the possibility of generating high frequencies using multiple vibrations in different phases. Under Condition 2, the doubled frequency component was dominant at all positions since pin vibrator vibrates in 60 Hz and the shape of the curve is M-shape. Under Condition 3, the PSD of the doubled frequency component was typically more dominant than that of the linear component at the gap that indicates the vibration overlap. Comparing the PSDs of doubled frequency component of Condition 2 and 3 in Figs. 7(b) and 8(b), the shapes of spatial distribution of doubled frequency components are significantly localized under Condition 3 which means, by overlapping small vibrations, the shape of the spatial distribution of doubled frequency can be typically shaped as a unimodal-shape and this distribution pattern cannot be achieved by a single pin-type vibrator. Pin vibrator with even detection threshold level vibration

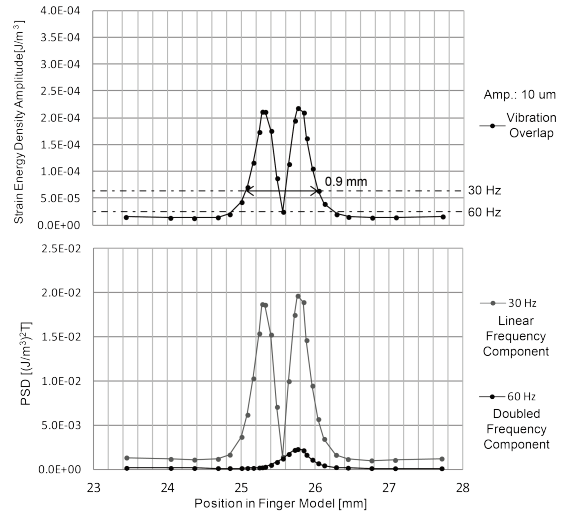


Figure 6. Condition 1: Vibration overlap with 10 $\mu$ m amplitude. (a)Upper: Spatial distributions of SED amplitude. (b)Lower: Spatial distributions of PSD.

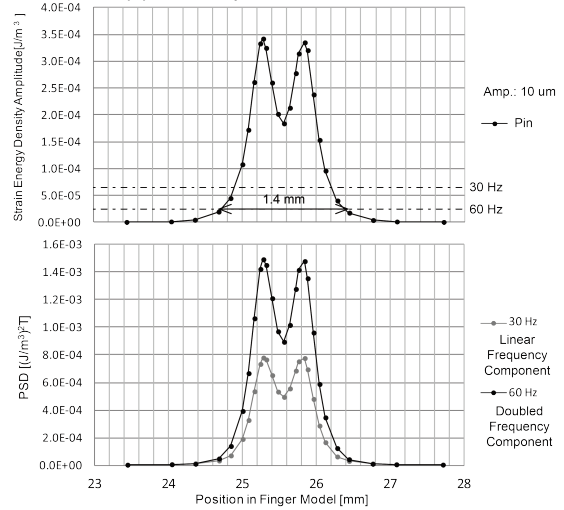


Figure 7. Condition 2: Pin-type vibrator with 10 $\mu$ m amplitude. (a)Upper: Spatial distributions of SED amplitude. (b)Lower: Spatial distributions of PSD.

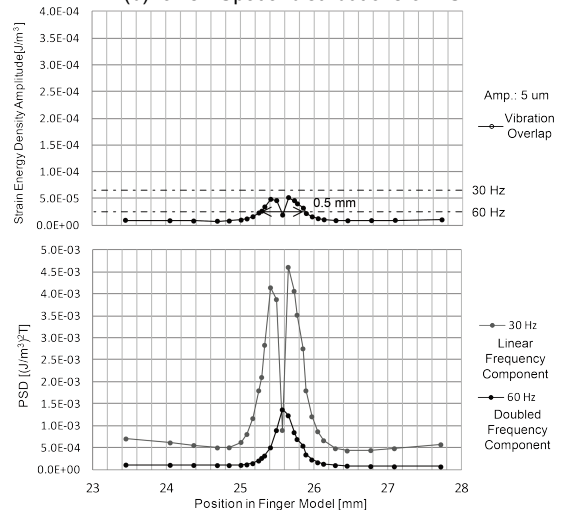


Figure 8. Condition 3: Vibration overlap with 5 $\mu$ m amplitude. (a)Upper: Spatial distributions of SED amplitude. (b)Lower: Spatial distributions of PSD.

generates wider spatial distribution of the doubled frequency components than vibration overlap method.

#### 4 ESTIMATION ON PERCEPTUAL AREA

In this section, we discuss how we estimated the perceptual area and determined the tactile image width considering the analysis results. We determined the threshold of the SED amplitude for perception and compared it with the deformation analysis results.

##### 4.1 Determination of deformation thresholds

In order to determine the SED amplitude threshold, we analyzed the basic mechanical condition for presenting vibration stimuli: applying vibratory stimuli with a flat surface vibrator. In this analysis, an 80 mm rigid surface was brought in contact with the FE finger model and vibrated at 30 and 60 Hz. The rigid surface was large enough to cover the entire area of the bottom of the finger model for the entire analysis time. Vibratory stimuli were generated according to eq. 1. The amplitude was set to each detection threshold level: 30  $\mu\text{m}$  for 30 Hz and 10  $\mu\text{m}$  for 60 Hz. The other analysis conditions were the same as those of the previous analysis in this study.

Fig. 9 shows the SED behavior average of each sample point for 30 and 60 Hz when the vibration of SED became stable. The SED amplitude threshold was  $6.21 \times 10^{-5} \text{ J/m}^3$  for the 30 Hz vibration and  $2.81 \times 10^{-5} \text{ J/m}^3$  for the 60 Hz vibration. These thresholds are drawn as dashed lines in Figs. 6(a), 7(a), and 8(a). We then adopted amplitude thresholds (30 or 60 Hz) corresponding to which frequency component was dominant at each position in the model.

##### 4.2 Discussion: Tactile Image Width

The SED amplitude thresholds and SED amplitude for each condition were compared to estimate the tactile image width. Under Condition 1, the SED amplitude was beyond the 30 Hz threshold, and the linear component was dominant in the spectral analysis result; thus, the tactile image width was 0.9 mm. Humans may perceive a 30 Hz vibration when the vibration overlap method is used with a large amplitude. Under Condition 2, the SED amplitude was beyond the 60 Hz threshold, so the tactile image width was 1.4 mm, which is larger than that for the vibration overlap method with the same amplitude (10  $\mu\text{m}$ ). Under Condition 3, the SED amplitude was smaller than the 30 Hz threshold; SED amplitudes beyond the 60 Hz threshold can be perceived. According to the spectral analysis, the doubled frequency component emerged at the gap, so the tactile image width was 0.5 mm. The tactile image was much smaller than that obtained using the pin vibrator. Human may perceive only the local doubled frequency vibration when using the vibration overlap method with an amplitude at the detection threshold level. This may be the reason for the sharp tactile sensation generated by the vibration overlap method.

#### 5 PSYCHOPHYSICAL EXPERIMENT

As the gap distance between two vibratory surfaces increases, the spatial distribution of the deformation changes and the detection thresholds for stimuli vary. We conducted a psychophysical experiment to investigate the effect of the gap distance on detection thresholds.

##### 5.1 Apparatus

Fig. 10 shows the experimental setup. A mechanical stage with a precision of 0.1 mm and a rigid stage were located on a base with sufficient area and weight. Piezoelectric actuators (TOKIN, AHB850C851FPOL-1F) were placed on these stages. These

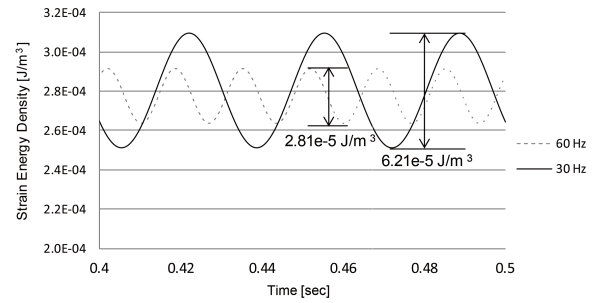


Figure 9. SED Amplitude thresholds for a flat contactor at 30 Hz and 60 Hz. The threshold was  $6.21 \times 10^{-5} \text{ J/m}^3$  for 30 Hz and  $2.81 \times 10^{-5} \text{ J/m}^3$  for 60 Hz.

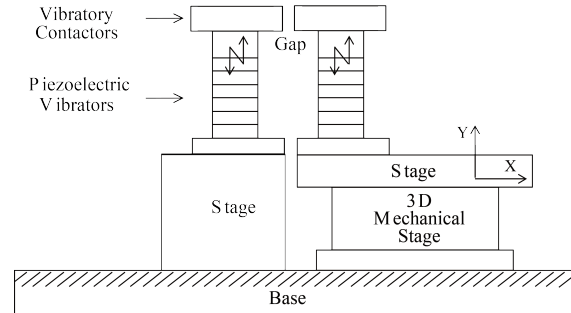


Figure 10. Experimental setup. Two vibrators vibrate in opposite phases, and the gap between them can easily be

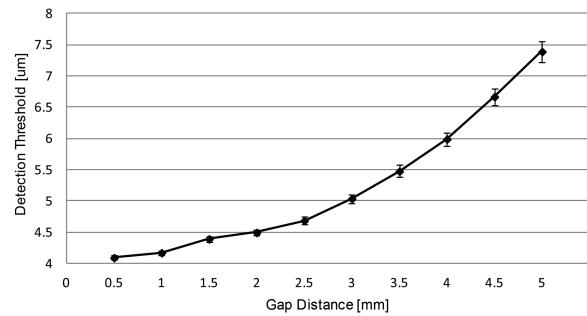


Figure 11. Experimental result: Detection threshold at each gap distance.

vibrators can provide amplitudes of more than 85  $\mu\text{m}$ , and the response frequency is greater than 400 Hz. Contactors were placed on the vibrators to regulate the size and shape of the contact area. The vibrators vibrate in opposite phases and generate a vibration overlap between the contactors. By tuning the jog of the mechanical stage, the gap distance can be easily changed.

##### 5.2 Methods

Subjects touched both vibratory contactors with their first finger to cover the gap with an indentation force of 1 N. Before the tests, subjects practiced touching the contactors with a 1 N force by touching a weight gage and adjusting the indentation force. The vibration amplitude of each vibrator was then simultaneously changed from 0  $\mu\text{m}$  to 85  $\mu\text{m}$ . The amplitude of the vibrations first recognized by the subjects was recorded. The amplitude was again changed from 85  $\mu\text{m}$  to 0  $\mu\text{m}$ , and the amplitude of the vibrations not perceived by the subjects first was recorded. The detection threshold was then calculated by the method of limits.

Under these conditions, the gap between the surfaces was increased by 0.5 mm for each trial. The gap distances used in this

study were 0.5, 1.0, 1.5, 2.0, 2.5, 3.0, 3.5, 4.0, 4.5, and 5.0 mm. The vibration stimuli followed eqs. 1 and 2. The frequencies were set to 30 Hz. Note that the stimuli were presented as the number of times the subject satisfactorily judged the presence of vibrations. Each trial was repeated twice, and the detection thresholds for five individuals were averaged. The subjects wore headphones that played pink noise so that they would not perceive any environmental changes. The five subjects were all right-handed males aged 21–28 years. None of the subjects had any known medical condition or disorders affecting their tactile sense.

### 5.3 Result

Fig. 11 shows the experimental result. Smaller gap distances meant that the detection threshold was lower. The vibration overlap method was effective for human sensitivity when the gap distance was small. The detection thresholds rose suddenly with gap distances of more than 2.5 mm. Note that in the previous test, we observed detection thresholds for gaps of less than 3.0 mm; the detection threshold curve was almost linear [8], and the results in this study do not contradict this knowledge. The feedback from the subjects indicated that the tactile sensation also differed at gaps of more than 3 mm: a sharp cutaneous sensation turned into a blunt shaking sensation.

### 5.4 Discussion

From the spectral analysis results and a comparison between the threshold and the deformation, humans may perceive only the doubled frequency component when the vibration overlap method is used with amplitudes at the detection threshold level. When the gap distance is increased, the doubled frequency component decays because the vibrations do not overlap. This phenomenon can be observed by comparing the detection thresholds for each gap distance in the psychophysical experiment: the detection threshold raise as the gap increases owing to the disappearance of the vibration overlap effect. In addition, it was reported from subjects that the tactile sensation changed as the gap increased. This may be due to the gradually disappearance of high frequencies by the overlapped vibrations.

Deformation and spectral analyses on larger gaps will be part of our future work.

## 6 SUMMARY

In this study, we investigated the mechanism behind the sharp tactile sensation produced by the vibration overlap method.

Deformation analysis on a FE finger model to observe the SED spatial distribution revealed that the SED spread is more localized with the vibration overlap method than with the thin pole (0.5 mm diameter) pin vibrator even if the amplitudes are the same. When using vibration overlap with the amplitude of the detection threshold level, the peak and width of the SED curve became significantly smaller than those obtained from pin vibrator. Spectral analysis indicated that the high-frequency vibration is generated above the very center of the gap between vibrations in opposite phases. The spatial distribution of the high-frequency component was localized significantly using the vibration overlap, and that localized unimodal-shape distribution pattern cannot be obtained by a single pin vibrator.

The results of tactile image estimation suggested that with the vibration overlap method, human perceive tactile sensation only in a localized area that high-frequency component exists and the area is much smaller than one produced by a single pin vibrator.

The psychophysical experiment indicated that there was a positive correlation between detection threshold and the gap

distance between two vibratory surfaces. The gradient of the curve suddenly rose when the gap distance was more than 2.5mm which means, vibration overlap method was effective for smaller gap distances.

### ACKNOWLEDGEMENT

This work was supported by JSPS Grants-in-Aid for Scientific Research Number 24.7234.

### REFERENCES

- [1] J. Bliss: "Dynamic Tactile Displays in Man-Machine Systems," IEEE Transactions on Man-Machine Systems, Vol.11, No.1, pp.58-65, 1970.
- [2] Ian R Summers, Craig M Chanter, Anna L Southall and Alan CBady: "Results from a Tactile Array on the Fingertip," In Proc. IEEE EUROHAPTICS, pp.26-28, 2001.
- [3] Bach-y-Rita P., Kaczmarek K. A., Tyler M. E. and Garcia-Lora J.: "Form perception with a 49-point electrotactile stimulus array of the tongue," A technical note. J. of Rehabilitation Research and Development, Vol.35, No.4, pp.427-430, 1998.
- [4] Ki-Uk Kyung, Ahn M., Dong-Soo Kwon and Srinivasan M. A.: "A compact broadband tactile display and its effectiveness in the display of tactile form," In Proc. IEEE EUROHAPTICS, pp.600-601, 2005.
- [5] Q. Wang and V. Hayward: "Compact, Portable, Modular, High-performance Distributed Tactile Transducer Device Based on Lateral Skin Deformation," In Proc. IEEE HAPTICS'06, pp.67-72, 2006.
- [6] Mohamed Benali-Khoudja, Moustapha Haféz, Jean-Marc Alexandre, Abderrahmane Khedda, and Vincent: "VITAL: A New Low-Cost Vibro-Tactile Display System" In Proc. IEEE International Conference on Robotics and Automation'04, Vol.1, pp.721-726, 2004.
- [7] Tae-Heon Yang, Sang-Youn Kim, Chong Hui Kim, Dong-Soo Kwon and Wayne J. Book: "Development of A Miniature Pin-Array Tactile Module using Elastic and Electromagnetic Force for Mobile Devices" Third Joint Eurohaptics Conference and Symposium on Haptic Interfaces for Virtual Environment and Teleoperator Systems, pp. 13-17, 2009.
- [8] T. Sakurai, M. Konyo and S. Tadokoro: "Enhancement of Vibrotactile Sensitivity: Effects of Stationary Boundary Contacts," Proc IEEE/RSJ International Conference on Intelligent Robots and Systems (IROS'11), pp.3494-3500, San Francisco, 2011.
- [9] T. Sakurai, M. Konyo and S. Tadokoro: "Presenting Sharp Surface Shapes Using Overlapped Vibrotactile Stimuli," Proc IEEE/RSJ International Conference on Intelligent Robots and Systems (IROS'12), pp. 3300-3307, Faro, 2012.
- [10] M. A. Srinivasan and K. Dandekar: "An Investigation of the Mechanics of Tactile Sense Using Two-Dimensional Models of the Primate Fingertip," Trans. ASME, J. Biomech. Eng, Vol.118, pp.48-55, 1996.
- [11] T. Maeno and K. Kobayashi: "Relationship between the Structure of Finger Tissue and the Location of Tactile Receptors (3rd Report, Results of Contact Analysis between a Finger and a Rough Plate)," Trans. of the Japan Society of Mechanical Engineers, Series C, Vol.65, No.636, pp. 3321-3327, 1999.
- [12] Y. Makino, N. Asamura and H. Shinoda: "Multi Primitive Tactile Display Based on Suction Pressure Control," Proc. IEEE 12th Symposium on Haptic Interfaces for Virtual Environment and Teleoperator Systems, (Haptic Symposium 2004), pp. 90-96, Chicago, 2004.